48th AIAA Aerospace Sciences Meeting Including the New Horizons Forum and Aerospace Exposition
4 - 7 January 2010, Orlando, Florida
AIAA 2010-1214

Influence of Unsteadiness on Thrust Measurements of Pulse Detonation Engines

Frank K. Lu,[1] Manuj Awasthi[2] and Dibesh D. Joshi[2]
University of Texas at Arlington, Arlington, TX 76019

The measurement of thrust of a pulsed detonation engine is complicated by the inherent unsteadiness. A dynamical model of the structure is first produced and its impulse transfer function is obtained. Next, the system dynamics are deconvolved in the frequency domain from the output using windowing and filtering to reconstruct the input. The results show that non-interfering pulses could be reconstructed well. However, the reconstructed input of interfering pulses is higher than the input.

I. Introduction

It is obvious that thrust is an important performance parameter for pulse detonation engines (PDEs).[1] Much of the discussion in [1] involves thrust estimates based on gasdynamics parameters. The actual measurement of thrust in a pulse detonation engine is, however, fraught with complications due to unsteadiness and the response of the structure to which the load cell is attached. The complication is partly due to extending conventional thrust measurement techniques to unsteady measurements. It can be noted that steady thrust measurements can be formulated using simple models which lead to accurate values. However, as the structure itself undergoes cyclic accelerations, this unsteadiness which can result in large interference loads must be accounted for.

Recently, unsteady force measurements in impulse facilities such as shock and gun tunnels have been developed.[2–17] These methods generally require identification of the system's dynamic parameters by experiment and finite element modeling. A technique for deconvolving the dynamic response of the structure from the actual thrust that is produced is developed. The method is tested using model functions and also against a simple impulse experiment. The general approach is to first obtain the impulse transfer function of the PDE in a dynamic calibration. This impulse transfer function is then modeled. The dynamic behavior of the system subjected to a sequence of pulses, simulating a PDE operation, is next modeled. It is assumed that the system dynamics of a thrusting PDE is the same as that of the dynamic calibration. Therefore, this model can be used to determine the thrust (input) from a load cell measurement through a deconvolution procedure.

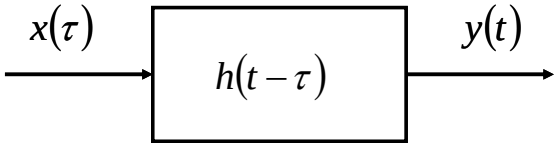

Figure 1. Block diagram for systems identification approach.

II. Method

In general, the method first requires the determination of the transfer function of the system $h(t)$ based on the input loading to the system is $x(t)$ and the output is $y(t)$, Fig. 1. For a linear system, one can write the relationship between the input, the output and the transfer function by the convolution[3]

$$y(t) = \int_0^t x(\tau)h(t-\tau)d\tau \tag{1}$$

If the input to the system is known, a deconvolution of Eq. (1) yields the transfer function. Once the transfer function is known, any arbitrary input can be determined from a measurement of the output.

An impulse (delta function)

$$x(t) = \delta(t) \tag{2}$$

[1]Professor and Director, Aerodynamics Research Center, Mechanical and Aerospace Engineering Department, Box 19018. AIAA Associate Fellow.

[2]Undergraduate Research Assistant, Mechanical and Aerospace Engineering Department, AIAA Student Member.

is commonly used for the input. Therefore,

$$y(t) = \int_0^t \delta(\tau) h(t-\tau) d\tau \tag{3}$$

Deconvolution of Eq. (3) in the time domain can be a tedious procedure. Thus, in order to obtain the transfer function, the analysis can be performed in the frequency domain and results can then be reverted back to the time domain. In the frequency domain, the transfer function of the system can be written as

$$H(s) = \frac{Y(s)}{X(s)} \tag{4}$$

From Eq. (4) the input in the frequency domain can be written as

$$X(s) = \frac{Y(s)}{H(s)} \tag{5}$$

where *H(s)* is impulse transfer function, *Y(s)* is the Fourier transform of the output and *X(s)* is the Fourier transform of the input. Once the output from an impulse is measured or calculated, the transfer function of the system can be determined using Eq. (4). Subsequently, Eq. (5) allows any input to be reconstructed if the output is known. In finite element analysis, the impulse can be simulated as a single triangular pulse of short duration.

III. Results and Discussion

A three-dimensional model, shown in Fig. 2, is used to simulate the dynamics. The model is a 2 ft long, AISI 306 steel pipe, with internal and external diameters of 0.75 and 1 in. respectively. The pipe is assumed to be free at the end at which force is applied and the other end is fixed. The fixed end is where the response is obtained, i.e., it is where in practice a load cell is mounted to measure the output from a PDE. The finite element model consists of 64 elements and 488 nodes. Natural frequencies and mode shapes of the pipe were obtained by performing a modal analysis. The time step for the unsteady analysis was chosen based on the highest frequency obtained from the modal analysis and is 0.1 ms.

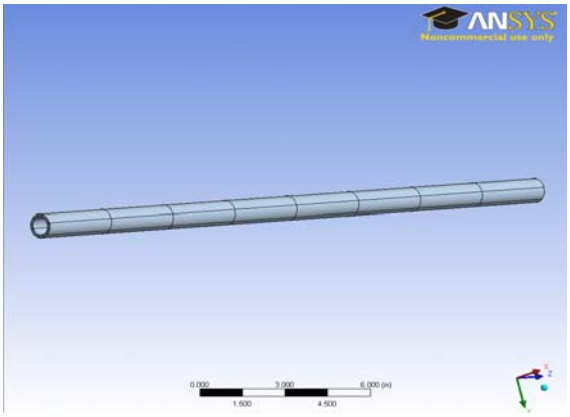

Figure 2. CAD model.

A. Impulse response

A triangular impulse is used to approximate the delta function as shown in Fig. 3. The peak is 100 lbf at 0.0001 s. The output displayed in Fig. 4 shows high-frequency ringing which damped out. From the output and the input, Eq. (4) then yields the transfer function, whose magnitude and phase spectra are shown in Fig. 5. Figure 5a shows a resonance peak at 3.967 kHz. The inverse transformation is then applied to the output to produce the reconstructed input as shown in Fig. 6. As highlighted above, once the transfer function is obtained, it can then be applied to other inputs.

B. Steady-state response

In the next test, a step load of 100 lbf is applied. The output is shown in Fig. 7 and it displays initial, large, high-frequency oscillations due to the response of the structure. Eventually, the oscillations damp away and the output settles to a steady value of 100 lbf. This output was then used to reconstruct a "raw" input $x'(t)$ through an inverse transform:

$$x'(t) = \int_0^t \frac{y(\tau) w(\tau)}{h(t-\tau)} dt \tag{6}$$

where the Tukey (or tapered cosine) window is used. This window is given in digital form by

$$w(n) = \begin{cases} 1 & 0 \le |n| \le \alpha N/2 \\ \frac{1}{2}\left[1+\cos\left(\pi \frac{n-\frac{\alpha N}{2}}{(1-\alpha)N}\right)\right] & \alpha N/2 \le |n| \le N/2 \end{cases} \tag{7}$$

where $\alpha = 0.05$ and the window length $L = N+1$. This window is one of a number with good side-lobe suppression behavior.[18–20] The raw reconstructed input is then subjected to a low-pass Butterworth filter with a cutoff frequency of 500 Hz. The result is displayed in Fig. 8 which shows that the procedure is able to reconstruct the steady-state input after an initial transient. It is not clear if the initial transient of the reconstructed input is due to the window or to the filter and is the subject of ongoing investigation.

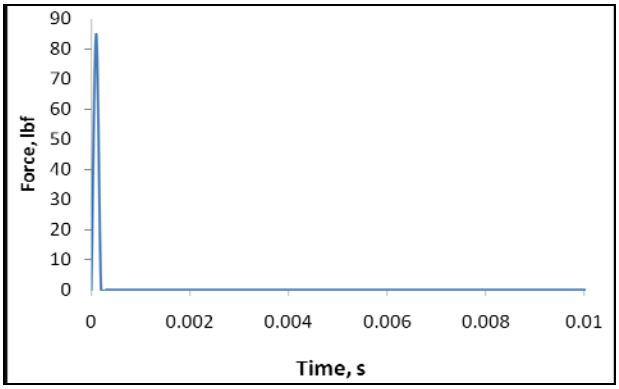

Figure 3. Triangular impulse input with a 100 lbf peak.

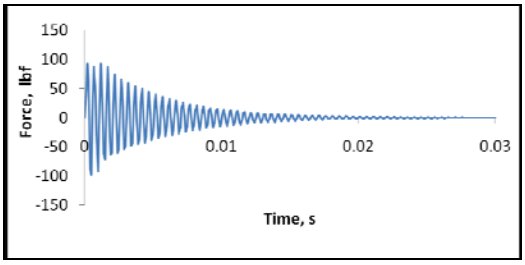

Figure 4. Response to triangular impulse.

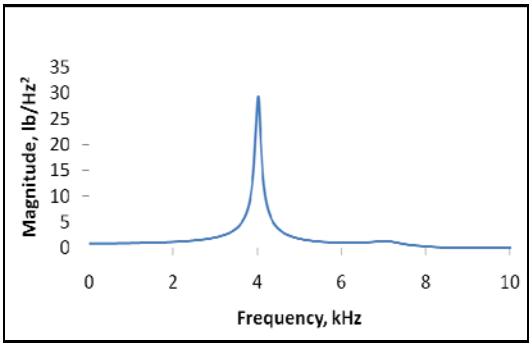

(a) Amplitude spectrum,

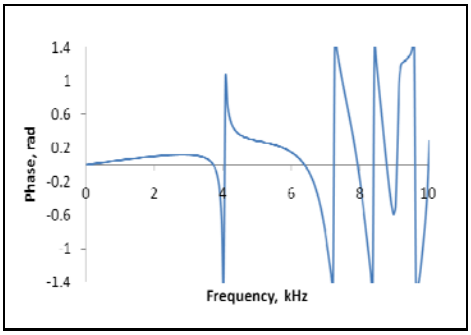

(b) Phase spectrum.

Figure 5. Triangular impulse input with a 100 lbf peak.

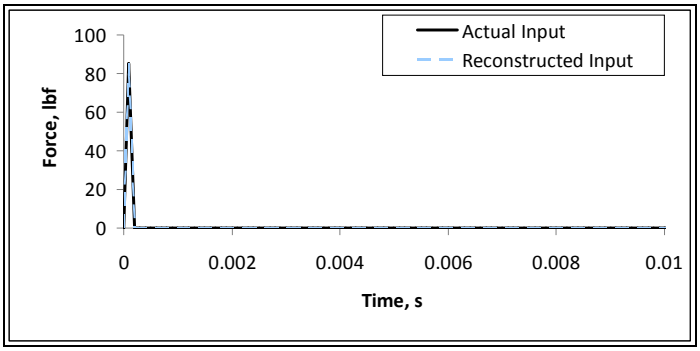

Figure 6. Reconstruction of input based on output and transfer function.

C. Single exponential decay

A single exponential decay function of the form

$$x = A\exp(-bt/100) \tag{8}$$

where $A = 85$ and $b = 4$ is used to simulate a detonation wave with a long Taylor rarefaction. The input and output are shown in Fig. 9 while the reconstructed output, following the procedure outlined above, is shown in Fig. 10. Figure 9 shows large oscillations in the output that does not appear to capture the input. Figure 10 shows the reconstructed input that appears closer to the actual input. The large oscillations at about 0.035 s may be attributed to the window.

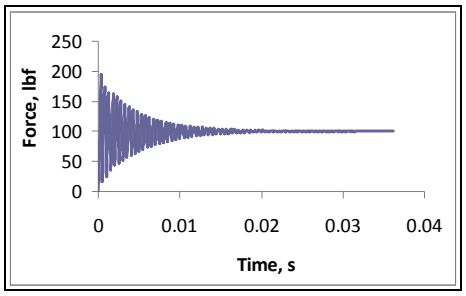

Figure 7. Output from a 100 lbf step input.

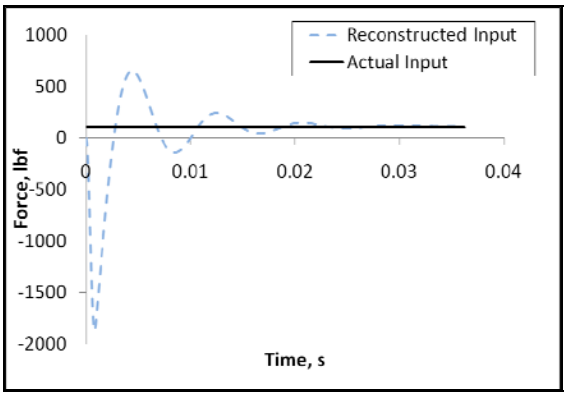

Figure 8. Reconstructed input.

D. A train of pulses

The output from a pulsed detonation engine is simulated by a train of exponential functions of the form given by Eq. (8). For illustrative purposes, five pulses at 50 Hz are reconstructed. The value of $b = 42500$ allowed the pulses to be considered to be non-interfering. Ten pulses are considered at 100 Hz with the value of $b = 2500$ to represent the case of interference between the detonation waves.

The output for the non-interfering case is shown in Fig. 11. Low-pass filtering the output does not yield satisfactory results as it removes the high-frequency information. However, the present reconstruction procedure with low-pass filtering at 10 kHz yields satisfactory results as shown in Fig. 12. The discrepancies at both ends between the input and the reconstructed input are due to wndowing effects. These effects can be corrected but not done so at present.

For the interfering case, the output shows excursions in excess of 100 lbf as shown in Fig. 13. Following the same reconstruction procedure, the reconstructed input is found to be about 10 percent above the actual input, as shown in Fig. 14. The reason for this discrepancy is unknown at the moment.

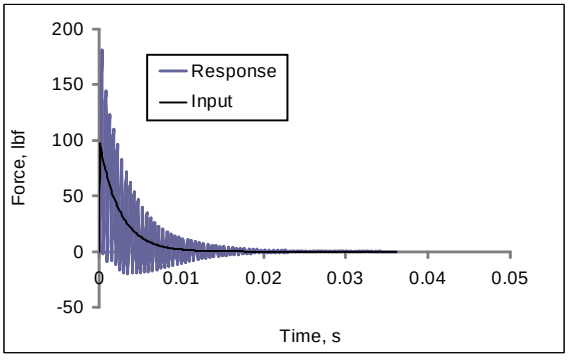

Figure 9. Output from an exponentially decaying input.

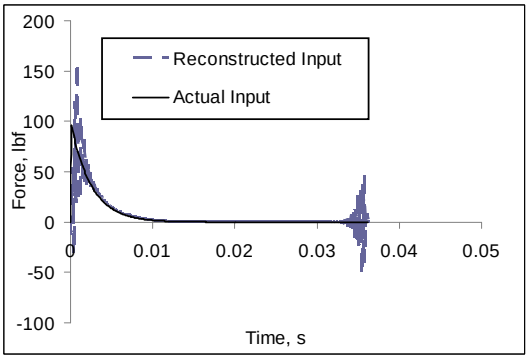

Figure 10. Reconstructed input.

IV. Conclusions

A method for obtaining the unsteady thrust of pulse detonation engines is proposed. The method utilizes a finite element model to obtain the structural dynamics from each the structure's impulse response can be obtained. Once the impulse response is known, a deconvolution procedure is applied to reconstruct the input. The method was tested against a step input, a single exponentially decaying input as well as a train of exponentially decaying pulses. In general, the reconstruction is good except for the interfering pulse train.

Future work will involve a comparison of different window functions to choose an optimal one. The technique will also be tested against model signals with noise. Finally, the technique will be applied to actual experiments. These involve a standard hammer test with a single or multiple strikes. Testing with actual detonations, single and multiple pulse, are also contemplated.

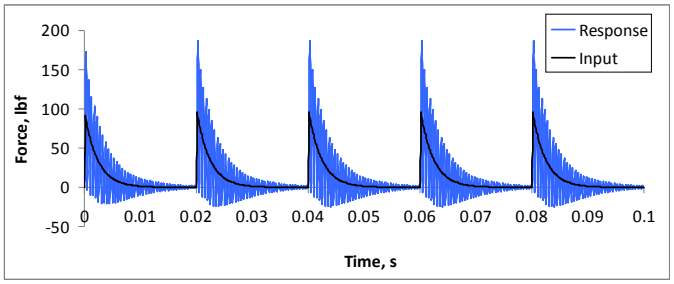

Figure 11. Response due to a train of non-interfering, exponentially decaying pulses

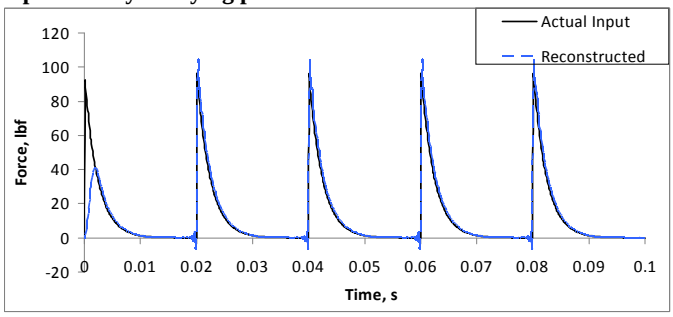

Figure 12. Reconstructed input.

References

[1] Kailasanath, K., "Recent Developments in the Research on Pulse Detonation Engines," *AIAA Journal*, Vol. 41, No. 2, 2003, pp. 145–159.

[2] Bernstein, L. "Force Measurement in Short-Duration Hypersonic Facilities," AGARDograph AGARD-AG-214, 1975.

[3] Naumann, K.W., Ende, H. and Mathieu, G., "Technique for Aerodynamic Force Measurement Within Milliseconds in Shock Tunnel," *Shock Waves*, Vol. 1, No. 3, 1991, pp. 223–232.

[4] Sanderson, S.R. and Simmons, J.M., "Drag Balance for Hypervelocity Impulse Facilities," *AIAA Journal*, Vol. 29, No. 12, 1991, pp. 2185–2191.

[5] Daniel, W.J.T., and Mee, D.J., "Finite Element Modelling of a Three-Component Force Balance for Hypersonic Flows," *Computers & Structures*, Vol. 54, No. 1, 1995, pp. 35-48.

[6] Smith, A.L. and Mee, D.J., "Drag Measurements in a Hypervelocity Expansion Tube," *Shock Waves*, Vol. 6, No. 3, 1996, pp. 161–166.

[7] Storkmann, V., Olivier, H. and Grönig H., "Force Measurements in Hypersonic Impulse Facilities," *AIAA Journal*, Vol. 36, No. 3, 1998, pp. 342–348.

[8] Sahoo, N., Mahapatra, D.R., Jagadeesh, G., Gopalakrishnan, S. and Reddy, K.P.J., "An accelerometer balance system for measurement of aerodynamic force coefficients over blunt bodies in a hypersonic shock tunnel," *Measurement Science and Technology*, Vol. 14, No. 3, 2003, pp. 260–272.

[9] Mee, D.J., "Dynamic Calibration of Force Balances for Impulse Hypersonic Facilities," *Shock Waves*, Vol. 12, No. 6, 2004. pp. 443–455.

[10] Joarder, R. and Jagadeesh, G., "A New Free Floating Accelerometer Balance System for Force Measurements in Shock Tunnels," *Shock Waves*, Vol. 13, No. 5, 2004. pp. 409–412.

[11] Sahoo, N., Suryavamshi, K., Reddy, K.P.J. and Mee, D.J., "Dynamic force balances for short-

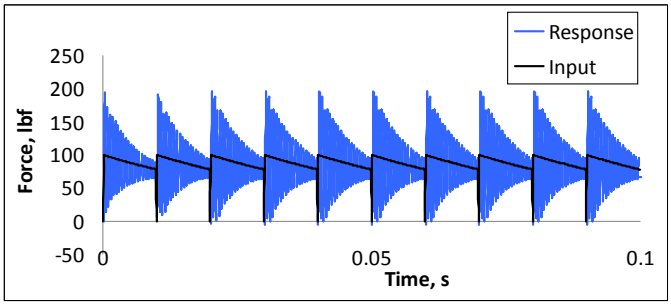

Figure 13. Response due to a train of interfering, exponentially decaying pulses

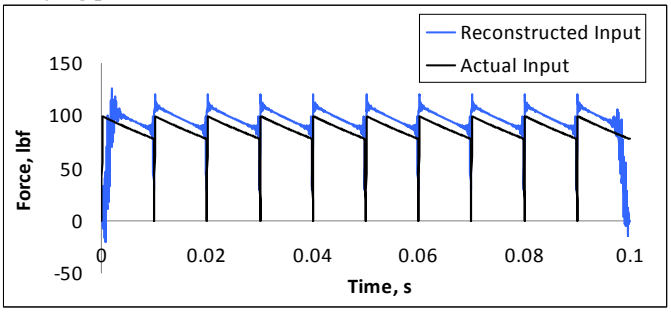

Figure 14. Reconstructed input.

duration hypersonic testing facilities," *Experiments in Fluids*, Vol. 38, No. 5, 2005, pp. 606–614.
[12] Tanno, H., Kodera, M., Komuro, T., Sato, K., Takahasi, M. and Itoh, K., "Aerodynamic Force Measurement on a Large-Scale Model in a Short Duration Test Facility," *Review of Scientific Instruments*, Vol. 76, 035107, 2005.
[13] Robinson, M.J., Mee, D.J. and Paull, A., "Scramjet Lift, Thrust and Pitching-Moment Characteristics Measured in a Shock Tunnel," *Journal of Propulsion and Power*, Vol. 22, No. 1, 2006, pp. 85–95.
[14] Sahoo, N., Mahapatra, D.R., Jagadeesh, G., Gopalakrishnan, S. and Reddy, K.P.J., "Design and Analysis of a Flat Accelerometer-Based Force Balance System for Shock Tunnel Testing," *Measurement*, Vol. 40, No. 1, 2007, pp. 93–106.
[15] Abdel-Jawad, M.M., Mee, D.J. and Morgan, R.G., "New Calibration Technique for Multiple-Component Stress Wave Force Balances," *Review Of Scientific Instruments*, Vol. 78, 065101, 2007.
[16] Ketsdever, A.D., D'Souza, D.C. and Lee, R.H., "Thrust Stand Micromass Balance for the Direct Measurement of Specific Impulse," *Journal of Propulsion and Power*, Vol. 24, No. 6, 2008, pp. 1376–1381.
[17] Satheesh, K. and Jagadeesh, G., "Analysis of an Internally Mountable Accelerometer Balance System for use with Non-Isotropic Models in Shock Tunnels, *Measurement*, Vol. 42, No. 6, 2009, pp. 856–862.
[18] Jenkins, G.M., "General Consideratitons in the Analysis of Spectra," *Technometrics*, Vol. 3, No. 2, 1961, pp. 133–166.
[19] Harris, F.J.., "On the Use of Windows for Harmonic Analysis with the Discrete Fourier Transform," *Proceedings of the IEEE*, Vol. 66, No. 1, 1978, pp. 51–83.
[20] Nuttall, A.H., "Some Windows with Very Good Sidelobe Behavior," *IEEE Transactions on Acoustics, Speech, and Signal Processing*, Vol. 29, No. 1, 1981, pp. 84–91.